

Design and synthesis of Janus micro- and nanoparticles

Adeline Perro,^{ab} Stéphane Reculosa,^b Serge Ravaine,^b Elodie Bourgeat-Lami^c and Etienne Duguet^{*a}

Received 12th April 2005, Accepted 28th June 2005

First published as an Advance Article on the web 25th July 2005

DOI: 10.1039/b505099e

Because the Roman god Janus was usually represented with two heads placed back to back, the term Janus is used for the description of particles whose surfaces of both hemispheres are different from a chemical point of view. So, they could be used as building blocks for supraparticular assemblies, as dual-functionalized devices, as particular surfactants if one hemisphere is hydrophilic and the other hydrophobic, *etc.* If they could allow the segregation of negative charges on one hemisphere and positive charges on the other one, they would display a giant dipole moment allowing their remote positioning by rotation in an electric field as a function of field polarity. This review deals with the great and imaginative efforts which were devoted to the synthesis of Janus particles in the last fifteen years. A special emphasis is made on scalable techniques and on those which apply to the preparation of Janus particles in the nanometer range. Specific properties and applications of Janus particles are discussed.

1 Introduction

Even though nanometric particles have been used in art since ancient times (*e.g.*, gold colloids dispersed in decorative glasses), considerable efforts have been devoted during recent years in the design, synthesis and understanding of their properties.¹ Various examples show that, on the nanometer scale, particles display original behaviours which are not observed in bulk materials and can be tuned by adjusting the particle size. Because of the minimization of interfacial tension energy, nanoparticles are typically prepared in spherical shape and their surface chemical groups are isotropically arranged. Theoretical works have shown that anisotropic particles could be very useful for controlling molecular recognition

and self-assembling processes, which are one of the more intriguing and challenging aspects in current materials science.² The synthesis of non-spherical nanoparticles is now

^aInstitut de Chimie de la Matière Condensée de Bordeaux, CNRS, Université Bordeaux-1, ICMCB/CNRS, 87 ave du Dr Albert Schweitzer, F-33608 Pessac, France. E-mail: duguet@icmcb.u-bordeaux1.fr; Fax: (+33) 540.002.761; Tel: (+33) 540.002.651

^bCentre de Recherche Paul Pascal, CNRS, Université Bordeaux-1, Pessac, France

^cLaboratoire de Chimie et des Procédés de Polymérisation, CNRS, CPE, Villeurbanne, France



Stéphane Reculosa

Stéphane Reculosa was born in 1977. He received an engineering diploma from the National School of Chemistry and Physics of Bordeaux in 2000. Since then he has carried out a PhD in physico-chemistry of condensed matter while studying the synthesis of materials with a controlled architecture based on colloidal silica particles, such as colloidal crystals or hybrid silica-polystyrene colloids with a well-defined morphology (and dis-symmetrical particles in particular). He received his PhD degree from the University of Bordeaux in 2004.



Adeline Perro

Adeline Perro was born in 1979. She received an engineering diploma from the National School of Chemistry and Physics of Bordeaux in 2003. She is currently carrying out a PhD on the elaboration of hybrid organic-inorganic nano-materials under the supervision of Professor Etienne Duguet and Professor Serge Ravaine at the University of Science and Technology of Bordeaux.



Serge Ravaine

Serge Ravaine received an engineer diploma from the National School of Chemistry and Physics of Bordeaux in 1991 and a PhD in Physical Chemistry at the University of Bordeaux in 1995. He is currently a full Professor at the University of Bordeaux and his research interests at the Centre de Recherche Paul Pascal in Pessac (France) include the synthesis of hybrid colloidal particles and the fabrication of three-dimensional colloidal photonic crystals.

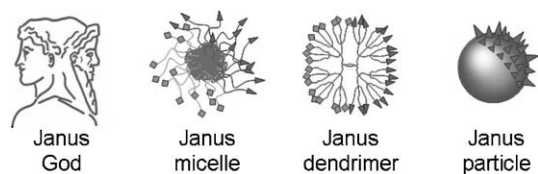


Fig. 1 Schematic representation of Janus-like morphologies compared to the dual-faced Janus god (Note: spheres symbolise particles; diamonds and triangles symbolise chemical functions).

a route which is extensively investigated.³ A complementary approach is the preparation of particles with diversely functionalised hemispheres. They could recognise themselves and select left from right, or top from bottom to yield supramolecular (or supraparticular) objects in a pre-programmed fashion, like proteins. In this way, a new chemistry based on nanoparticles instead of atoms could be imagined.⁴ Such a behaviour, combined to the specific physical properties of nanoparticles (*e.g.*, optical, magnetic, *etc.*), affords unique opportunities to create revolutionary material combinations.²

In 1991, on the occasion of his Nobel lecture, De Gennes was one of the first scientists to use the term Janus for the description of particles whose surfaces of both hemispheres are different from a chemical point of view (Fig. 1).⁵ In the Roman religion, Janus was the god known as the custodian of the Universe. He was usually represented with two heads placed back to back so that he might look in two directions at the same time. By considering Janus grains (*e.g.*, glass beads) displaying simultaneously polar and apolar faces, De Gennes described their spontaneous monolayer arrangement for instance at air/water interface.^{6,7} In comparison with similar films made of conventional molecular surfactants, he predicted promising properties due in particular to the presence of interstices between the grains and therefore to the possibility of

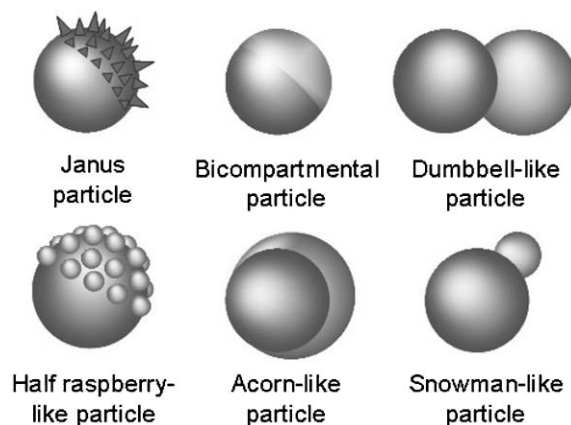


Fig. 2 Schematic representation of Janus and comparable particles (Note: spheres and diamonds symbolise particles and chemical functions, respectively).

chemical exchanges between water and air. He illustrated this property with the sentence: “The skin can breathe”.

During the last fifteen years, the “Janus” term has been also used for describing asymmetric dendritic macromolecules⁸ or unimolecular micelles based on block copolymers in solution (Fig. 1).⁹ Nevertheless, the present review will focus on hard and permanent Janus structures, *i.e.*, particles according to the original definition of De Gennes, and their asymmetry will be essentially considered from the viewpoint of their surface chemical groups. That is why, biphasic particles such as bicompartamental, dumbbell-like (hetero-doubelets or asymmetric dimers), snowman-like, acorn-like and half-raspberry-like particles will be also considered (Fig. 2). Indeed, they belong to the larger family of “dis-symmetrical particles”, where the asymmetry is also related to their shape and/or the chemical composition of their bulk.¹⁰



Elodie Bourgeat-Lami

Elodie Bourgeat-Lami is Research Director at CNRS. She received an engineering diploma from the National School of Chemistry of Mulhouse (France) in 1988 as well as a doctorate from the University of Montpellier II, Sciences et Techniques du Languedoc (France) in 1991. Just after finishing her doctorate, she joined CNRS in the team of Dr Alain Guyot. Currently, she is working in the Laboratory of Chemistry and Polymerization Processes

(LCPP) headed by Dr R. Spitz and located at the Ecole Supérieure de Chimie Physique Electronique de Lyon (CPE) in Villeurbanne, France. Her research interests are focused on the fundamental and practical aspects involved in the synthesis of organic–inorganic colloidal materials with special emphasis on radical polymerization in dispersed media (emulsion, dispersion and mini-emulsion polymerizations), surface functionalization of mineral oxide particles and sol–gel chemistry. Her



Etienne Duguet

research also includes activities on the synthesis of novel hybrid macromolecular architectures through living free radical polymerization as well as on the grafting of polymers to mineral surfaces using the grafting-to and grafting-from techniques.

Professor Etienne Duguet was born in 1965. He received an engineering diploma from the National School of Chemistry and Physics of Bordeaux in 1988 and a PhD degree in

polymer chemistry from the University of Science and Technology of Bordeaux in 1992. He is currently a full Professor and his research at Institute of Condensed Matter Chemistry of Bordeaux focuses on the synthesis of hybrid organic–inorganic materials based on inorganic particles derivatized through molecular surface modification, polymer encapsulation, dis-symmetrization and/or functionalisation for optical or medical applications.

Beyond their use as elementary building blocks for supraparticular assemblies as already mentioned, Janus particles should be very promising with respect to numerous applications.

By combining a hydrophilic hemisphere with a hydrophobic one, amphiphilic Janus particles could be useful for the stabilization of water-in-oil or oil-in-water emulsions.¹¹ About a century ago, Pickering discovered that fine solid particles could be used as stabilizers in emulsion technology.¹² Recently, it was shown that particles of intermediate hydrophobicity are most effective in stabilizing oil or water drops of submicron diameter for periods exceeding several years.¹³ Theoretical considerations predicted that desorption energies of homogeneous particles may be increased 3-fold by maximizing the amphiphilicity of Janus particles, which could prove to be efficient emulsion stabilizers.¹⁴ Therefore, in water-based paints for instance, Janus particles could play the role of surfactants during storage and application prior to become a conventional coating pigment. Specific arrangements of the amphiphilic pigments in the coating thickness would be expected allowing leafing or not-leafing effects.

If Janus particles were made of surface chemical groups allowing the segregation of negative charges on one hemisphere and positive charges on the other one, they would display a giant dipole moment allowing their remotely positioning by rotation in an electric field as a function of field polarity.¹⁵ If these dipolar particles were also bichromal, for instance, they could be used for electronic displays, such as the electronic reusable paper.¹⁶

As a last example of this non-exhaustive list of expected properties and applications, Janus particles displaying hemispheres coated with different chemical groups could be toposselectively functionalised by using the right antagonist reagents. So, they could be derivatised into original bifunctional carriers useful for catalysis, sensing, drug delivery, *etc.*

One of the main intentions of this contribution is to impart information about the great and imaginative efforts which were devoted to the synthesis of Janus particles in the last fifteen years. A special emphasis will be made on scalable techniques and on those which apply to the preparation of Janus particles in the nanometer range. Specific properties and applications of Janus particles will be discussed as fast as their synthesis will be described.

In the most general case, Janus and comparable particles are prepared from symmetric ones.¹⁰ Several dis-symmetrisation procedures, *i.e.*, chemical or physico-chemical processes altering the symmetry elements of the precursor particles, have been investigated. They can be classified in four general routes: techniques based on (i) toposelective surface modification, (ii) template-directed self assembly, (iii) controlled phase separation phenomena and (iv) controlled surface nucleation. The first route reported in the next section is the exception which proves the rule, because as far as we know it is the single route allowing to prepare Janus particles in a one-step process.

2 The dual-supplied spinning disk technique

This original technique allows the one-step synthesis of bicompartamental polymer particles.¹⁶ Molten white and black wax-like polymers are introduced on opposing sides of a disk, which is spinning at around 2700 rpm, where they flow to the edge and form small jets which are black on one side and white on the other one (Fig. 3a). Due to the Rayleigh instability, they break up into 100- μm bichromal balls which quickly solidify as they fly through the air (Fig. 3b). The higher the spin, the higher the percentage of small beads. Depending on the nature of polymers, the two-tone balls display also a slightly stronger positive and permanent electric charge on one hemisphere than on the other one. Red/white, green/white, black/yellow and red/yellow balls can be also prepared by changing the nature of the colouring pigments in the wax-like polymers.

These bichromal beads are used in the Gyricon display medium (from the Greek root *gyro*, to rotate, and *icon*, image) that combines the advantages of paper with electronic addressability.¹⁷ Ten of thousands of microballs are blended with uncured elastomer, which is converted to a sheet 250 to 500 μm thick prior to curing. The sheet is then soaked in a low viscosity silicon oil to make it swell and form cells of oil around each ball, which is now free to rotate when exposed to an electrical field. The sheet is sandwiched between sheets of plastic which carry a grid of addressing electrodes similar to those used in conventional liquid crystal displays (Fig. 3c). This arrangement provides the switching circuit to control the ball rotation. Applying one polarity of field (± 50 V) gets a white hemisphere display; the opposing polarity displays black hemispheres. If a precise enough charge is transmitted, one to

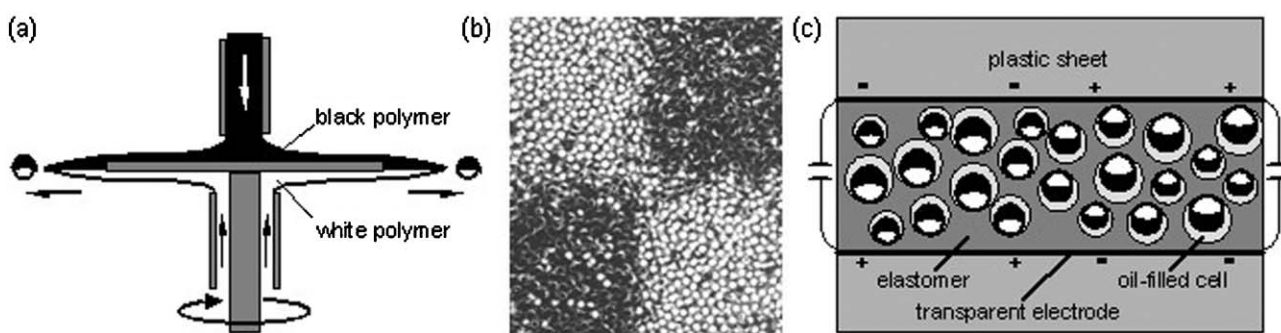


Fig. 3 The Gyricon rotating ball display: (a) the dual-supplied spinning disk apparatus for the fabrication of bichromal balls, (b) 100- μm black/white balls as organised on the corners of squares imaged with the Gyricon display, (c) schematic cross section of the Gyricon display medium. Reprinted and redrawn from www.gyricon.com.

each encapsulated sphere for an independent response, the spheres are impacted against the wall of their cell, where they stay until dislodged by another electrical field. Forty-cm square displays were built at a resolution of 220 dots per inch. Next challenges concern a higher resolution, a truer white image and therefore smaller and more tightly packed balls.

3 Processes based on toposelective surface modification

The toposelective surface modification of precursor symmetric particles is the most intuitive route to elaborate site-specific functionalised Janus particles. The main challenge is to modify one hemisphere without altering the surface of the other one. The reported strategies are: (i) the temporary masking of one hemisphere during the surface modification of the other one, (ii) the use of reactive directional fluxes or fields supposing that the particle screens the face which shall not be modified, (iii) the microcontact printing, (iv) the partial contact with a reactive medium thanks to the arrangement of the particle along an interface on the assumption that the particle is unable to rotate during the procedure (Fig. 4).

(a) Surface modification of partially-masked particles

This is the oldest way to obtain Janus particles. The very first example was mentioned by De Gennes in 1991 and, in fact, it had been reported by his colleagues in 1988. They described the elaboration process of amphiphilic glass microspheres (40–50 μm in diameter) and the study of their behaviour at water/oil interfaces.^{6,7,18,19} The commercial precursor beads were deposited on a solid substrate covered with a cellulose varnish film of controllable thickness partially protecting the particles. The unprotected hemispheres were treated with

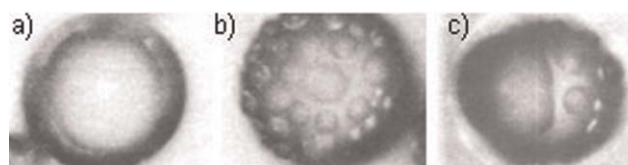


Fig. 5 Optical microscopy images displaying discriminatory water condensation on an amphiphilic Janus glass bead. (a) Hydrophilic face, (b) hydrophobic face, (c) mixed face. Reprinted with permission from ref. 18.

octadecyltrichlorosilane to make them hydrophobic, whereas the protected ones remain hydrophilic. After dissolution of the varnish, the glass beads were released, washed and dried. Their amphiphilic character was checked by optical microscopy experiments which showed a discriminatory behaviour of water vapour with the formation of small droplets onto the hydrophobic hemispheres (droplets diameter of about 10 μm ; contact angle around 90°) and a continuous film onto the hydrophilic one (Fig. 5).

The behaviour of these amphiphilic Janus particles at the interface between water and different oils was studied and compared to that of totally hydrophilic or hydrophobic beads.^{6,19} It was observed under an optical microscope that all the beads were arranged along the interface, but the hydrophilic particles were preferentially immersed in the water phase, the hydrophobic ones in the oil phase and the amphiphilic Janus ones were symmetrically positioned at the interface. Such behaviour was explained on the basis of the different forces which act on the particles and considering that the total energy of the system is the sum of two contributions: one corresponds to the interfacial energy between the solid and the liquids and the other to the energy of the liquid/liquid interface. Later, theoretical studies were dedicated to such behaviour and predicted the effects of the hydrophilic and hydrophobic area ratio¹⁴ and particle shape.²⁰

Although interesting for large particles, the protecting-varnish technique is, however, unsuitable for nanoparticles, because control of the varnish layer thickness below 1 μm would be rather difficult. The selective patterning of 1- μm silica spheres using a photoresist layer was developed by the Bell Laboratories.²¹ A polished silicon wafer was covered by spin-coating with a monolayer of non-contacting silica beads from a colloidal solution and heat treatment at 250 °C to ensure a good adhesion between the particles and the substrate. The photoresist was then spin-cast and subsequently treated by a reactive ion etching plasma in order to reduce its thickness at a value lower than the silica bead diameter, therefore releasing a controlled area of the silica surface. Then, thin non-continuous layers of metal (Ti, Au, Ag or Cu) or metal oxide (Al_2O_3 or TiO_2) were deposited using e-beam sputtering, prior to remove the photoresist layer by soaking in a solvent. So, silica beads with metal or metal oxide caps may be prepared through this process, which is claimed to be useful for patterning spheres down to 100 nm in diameter. The authors also demonstrated that gold caps may be selectively derivatised with alkanethiols.

The last example of surface modification of partially-masked particles was recently reported as a gel trapping

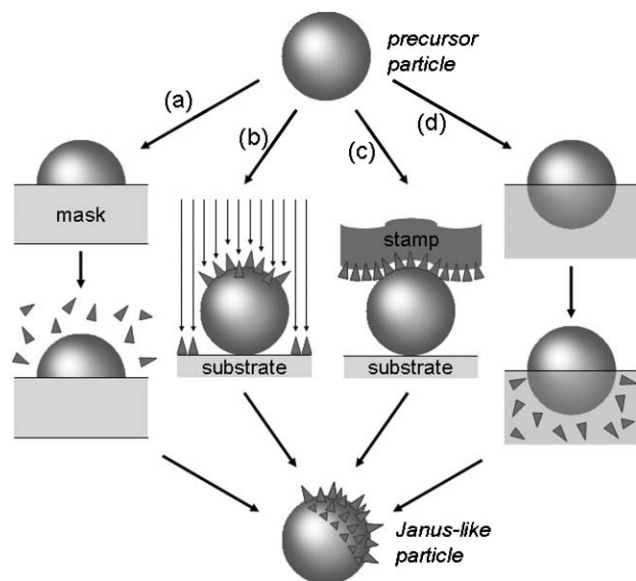


Fig. 4 Schematic representation of the four strategies allowing to toposelectively modify the surface of particles: (a) masking/unmasking techniques, (b) techniques using reactive directional fluxes or fields, (c) microcontact printing techniques and (d) techniques based on interfaces and partial contact with a reactive medium.

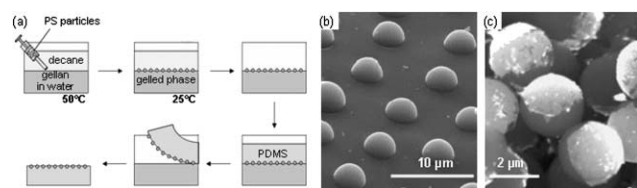


Fig. 6 (a) Schematic diagram of the gel trapping technique, (b) SEM image of 3.9 μm PS latex particles as arranged on the cured elastomer surface, (c) SEM image of Janus particles fabricated by gold sputtering on a monolayer of 2.7 μm sulfate PS latex particles partially embedded on the elastomer surface. Reprinted in part with permission from ref. 23.

technique.^{22,23} The first step is based on the injection of a colloidal dispersion of polystyrene (PS) particles at the interface between a hot hydrocolloid aqueous solution (gellan 2 wt%) and a pre-warmed decane phase (Fig. 6a). After gelling the water subphase at room temperature, the decane phase was replaced by polydimethylsiloxane (PDMS) oil which is cured for 48 h. Then the solid elastomer was peeled off the gel and the particle monolayer trapped on the gel surface is therefore replicated and transferred onto the elastomer surface. By a simple scanning electron microscopy (SEM) observation, this method allowed the measurement of the three-phase contact angle of the particles adsorbed at the oil/water interface (Fig. 6b). In a further step, gold was evaporated onto the elastomer surface and the gold-capped PS particles were mechanically recovered from the substrate (Fig. 6c). According to the authors, the gel trapping technique is efficient for the dis-symmetrisation of particles down to 100 nm in diameter.

(b) Surface modification of particles in directional fluxes and fields

In this part, the surface modification of one hemisphere of the particles is performed in reactive directional fluxes. The second hemisphere is supposed to be spared the reaction because it is sheltered by the particle itself. This route allows avoiding the tedious masking and unmasking steps.

An easy method was reported to prepare Janus particles by evaporating gold on particles (diameter of 20–50 μm).¹⁵ By so-treating one single hemisphere of fluorescent latex microspheres which were negatively charged, the authors were able to functionalize this gold cap with either 2-aminoethanethiol or thioglycolate to bring positive charges on this hemisphere and create a giant dipole moment. As shown on Fig. 7a, the deposited gold layer is sufficient to quench fluorescence and discriminate both hemispheres under a fluorescence microscope. Moreover, the electric dipole moment of these Janus particles appeared to be pH-dependent. When subjected to an alternating electric field in various buffer solutions, their electrophoretic rotation as a function of the direction of the electric field was monitored by fluorescence microscopy (Fig. 7). Such fluorescent colloidal particles show intensity fluctuation (blinking) because of their rotational Brownian motion.²⁴ Interactions between molecules immobilised on the surfaces of the particle and the solid substrate restrict the rotation of the particle, thus modulating the intensity

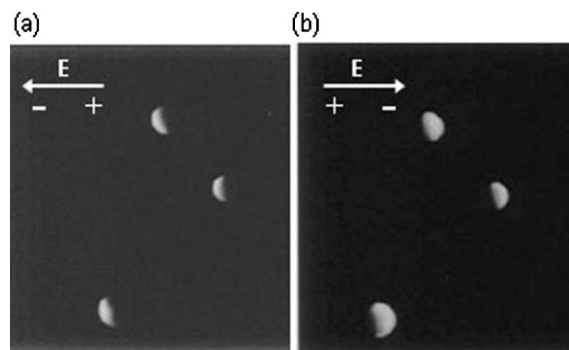


Fig. 7 Electrophoretic rotation of 20 μm fluorescent latex particles partially recovered of gold and modified with 2-aminoethanethiol. Fluorescence was quenched by evaporated gold, allowing for ready observation of rotation. The polarity of the electric field was reversed between the two shots. Reprinted with permission from ref. 15. Copyright 1997 American Chemical Society.

fluctuations. Because the time-dependent rotational angle can be obtained from the fluorescent intensity, the intensity signals can be used to investigate the weak interactions between unlabelled molecules by analysing the angular distribution of the particle. This study was the first demonstration of an optical measurement of the particle rotations.

The usefulness of golden Janus nanoparticles monolayers was investigated for an optical sensor device.²⁵ They showed with PS latex particles of 110 nm that the resulting sample exhibited a large extinction coefficient of optical density of 2.4 with a bandwidth of 100 nm in the visible region. The extinction peak position was found to depend linearly on the refractive index of the environment. They demonstrated that formation of a thiol monolayer can be detected *in situ* and that biological binding as modelled by the biotin–avidin pair can be detected without labelling. The sub-monolayer sensitivity of this device promises development of optical biosensors which could be readily incorporated into microfluidic devices or single-use disposable kits.

This technique of metal evaporation may obviously be applied to particles of different nature in a wide range of size. Nevertheless, a more recent study demonstrated that for diameters less than 100 nm, a thorough control of the metallic film thickness is necessary for avoiding dis-symmetrised particles that were stuck together.²⁶ When the precursor particles are silica beads, and providing that a preliminary Ti–W adhesion layer was deposited before the gold one, an annealing step in air at 700 $^{\circ}\text{C}$ for 3 h allows the gold cap to dewet and form a gold microcrystal on top of each individual silica bead (Fig. 8a).²⁷ So, half raspberry-like or halfmoon-like particles may be easily converted to snowman-like particles. For specific purposes, silica particle may be dissolved in an aqueous HF solution for the production of gold half-shells with diameters ranging from 100 to 500 nm and shell thickness of 8–15 nm (Fig. 8b).²⁸ By varying the nature of the evaporated metal, platinum or palladium half-shells were also fabricated.

As a last application example of gold–silica Janus particles, their possible use as dual-functionalised building blocks in a preliminary step towards selective DNA-directed assembly

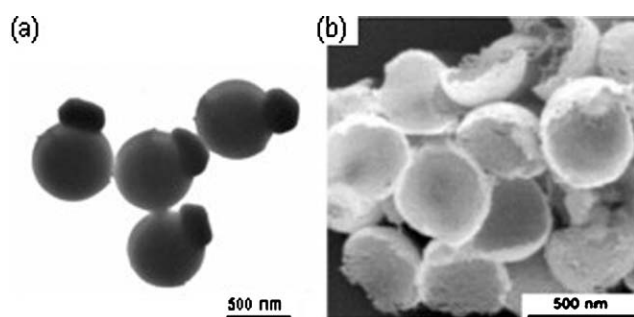


Fig. 8 (a) Snowman-like silica-gold particles as formed by dewetting half-shells of gold deposited on one hemisphere of silica precursor particles. Reprinted with permission from ref. 27. (b) Gold half-shells obtained from acorn-like silica-gold particles after dissolution of the silica template. Reprinted in part with permission from ref. 28. Copyright 2003 American Chemical Society.

was recently reported.²⁹ The authors took advantage of the biphasic nature of the particles for performing two non-interfering chemical procedures: silane chemistry was chosen for the silica side and thiol chemistry for the gold side. So, they immobilised different oligonucleotide sequences on each of the two hemispheres (Fig. 9a). These dual-functionalised microspheres were used in the selective orthogonal assembly of fluorophore-tagged target oligonucleotides. The chemistry efficiency and selectivity were checked by confocal microscopy (Fig. 9b). Further experiments are currently in progress for assembling these building blocks into highly complex hierarchical structures.

On the occasion of the preparation of electrodeposited catalysts, a method for topospecifically depositing catalytically active metals (Au, Pd) onto electrically conducting particles (graphite) using electric fields was developed.³⁰ An acetone suspension of graphite particles (diameter of 1–2 μm) was nebulized onto a thick cellulose paper. The papers were then stacked together and sandwiched between two flat graphite electrodes. After immersion in a toluene-acetonitrile solution of PdCl_2 , the application of an electric field polarized the electrically isolated graphite particles and resulted in separate anodic and cathodic regions on the same particle. Then the reduction process involves the electrodeposition of the metallic Pd. The transmission electron micrograph shows a graphite particle to which Pd and Au were applied sequentially to opposite ends by reversing the direction of the electric field. Such a particle may be assimilated to a Janus-like object, with the additional characteristics that both faces are not only chemically different but also different from those of the pristine particle.

Lastly, recent results demonstrated the possibility to “smartly” make the surface of silica microparticles dissymmetrical by a laser photochemical deposition process.³¹ It consists of an extension of the lithographic techniques developed so far on spherical and confined surfaces onto planar and cylindrical substrates. Micron-sized silica beads (10 μm in diameter) were first immobilized in an acidic hydroalcoholic solution of Cr(VI) ions in a glass cell of 30 μm -thickness in the direction of the laser beam. The photoreduction reaction of Cr(VI) to Cr(III) is driven in

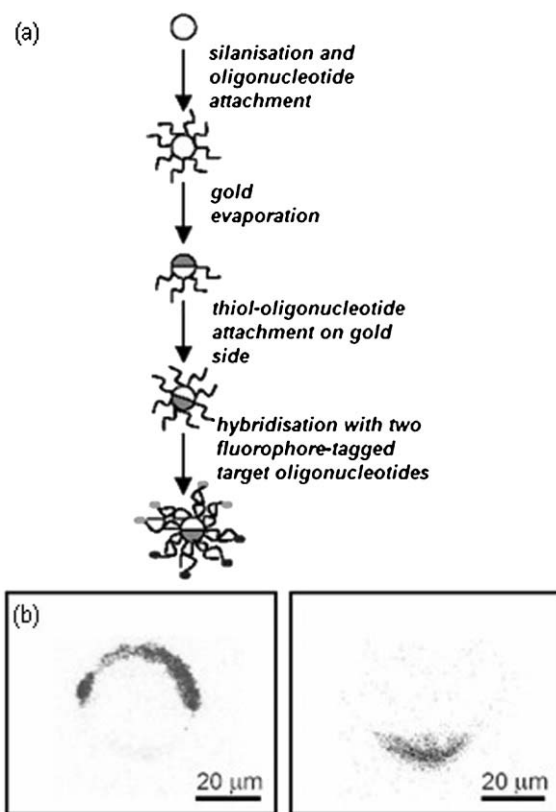


Fig. 9 (a) Schematic representation of the overall process of preparing the dual-functionalised particles and demonstrating the orthogonal assembly of fluorophore-tagged complementary oligonucleotides. (b) Confocal microscopy images of the cross-section of one dual-functionalised particle after hybridisation with target oligonucleotides tagged with tetramethylrhodamine for the silica hemisphere and Cy5 for the gold hemisphere. The left image corresponds to tetramethylrhodamine signals obtained with a 543 nm laser excitation and the right image corresponds to Cy5 signals at 633 nm. Reprinted with permission from ref. 29.

the blue-green wavelength (514 nm) by an Ar^+ laser, of which the incident beam power may be adjusted. Through the use of an optical microscope, the beam has to be previously focused on the top hemisphere of a bead. Fig. 10 shows the growth of the Cr(OH)_3 cap onto the silica surface. Nevertheless, this technique, which allows also a micro-patterning *via* a computer-monitoring of the cell holder, is limited to microparticles because of the optical resolution.

(c) Surface modification of particles through microcontact printing

The third way to topospecifically modify one hemisphere of particles is derived from the microcontact printing technique, which is an easy and efficient way to produce patterns of self-assembled monolayers even of sub-micrometer lateral dimensions. It is assumed that only the surface of the contact area of the particles with the elastomer stamp is modified.

First experiments were dedicated to the preparation of dipolar Janus particles through the microcontact printing of water-insoluble cationic surfactants (*e.g.*, octadecyltrimethylammonium) onto monolayers of negatively-charged sulfate PS

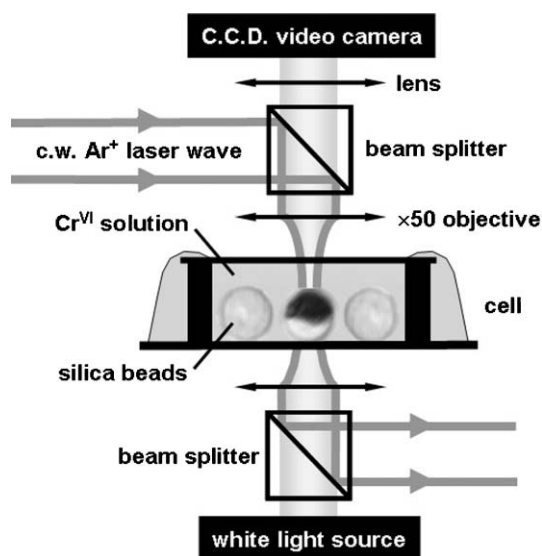


Fig. 10 Schematic representation of the experimental setup implemented for the preparation of laser-induced Janus particles by photochemical deposition of chromium hydroxide onto 10- μm silica beads centered in the beam. Reprinted with permission from ref. 31. Copyright 2003 American Chemical Society.

latex particles.³² The first step is the preparation of the particle monolayer by evaporation of a latex suspension spread on a glass substrate (Fig. 11a). A surfactant film is deposited on hydrophilised elastomer stamp. Then the particle monolayer is stamped with the surfactant film and the so-polarised particles are redispersed in water. At high salt concentrations, the repulsion due to the net surface charge is suppressed and orientation effects due to dipole-dipole interactions take place and lead to the formation of primarily linear aggregates. When the surfactant is replaced by a fluorescent lipid, *e.g.*, rhodamine-tagged lissamine, the dis-symmetry of the particles may be directly observed under a fluorescence microscope (Fig. 11b). For a better control of the area fraction in contact with the flexible elastomer stamp, the particle monolayer may be partially embedded into a protective film of glucose. The same authors prepared half raspberry-like particles through a similar process by arranging small sulfate latex particles onto the stamp and larger aminoalkyl latex particles onto the glass substrate.³³

A last example was recently reported for the synthesis of snowman-like particle arrays for anti-reflecting surfaces.³⁴ It is now admitted that fabrication of surface relief structures is one of the most promising way for achieving low surface reflectivity. In particular, the array of conical protuberances with sinusoidal profiles cause efficient variations in the refractive index between the air and substrate to be gradual.³⁵ These structures are commonly referred to as “motheys” structures, because they mimic the geometry of the corneal lenses of night-flying moths. The microcontact printing route was used for depositing a cationic polyelectrolyte of poly(allylamine hydrochloride) onto an array of negatively-charged 100-nm PS latex particles arranged onto a glass substrate. Then, similar but smaller (50 nm) latex particles were let to adsorb onto the array. For electrostatic reasons,

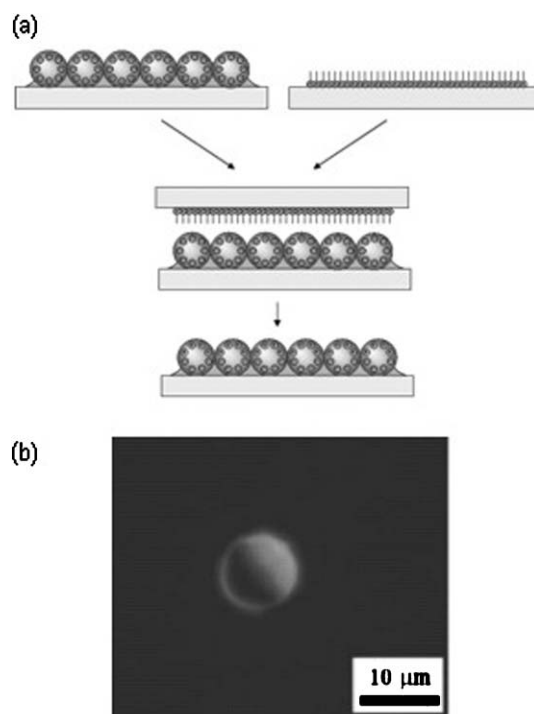


Fig. 11 (a) Schematic representation of the overall process of making dipolar Janus particles by microcontact printing of a surfactant film onto a monolayer of oppositely charged latex particles. (b) Fluorescence microscopy image of 9.6- μm PS latex particles stamped with fluorescent rhodamine-tagged lissamine. Reprinted with permission from ref. 32.

they arranged essentially onto the top cap of the larger particles in a snowman-like morphology (Fig. 12a). The substrates remained optically transparent and the transmittance was measured at normal incidence over the visible spectral range. Transmission spectra showed that these particle-on-particle patterns clearly increased light transmittance compared to uncoated glass and particle monolayers (Fig. 12b). They caused a red shift of about 50 nm in the maximum transmission wavelength and showed an enhanced transmittance (up to 97.8%) at this wavelength. Further efforts will concern the control over the placement and periodicity of the particles, in order to match the simulated spectra (inset of Fig. 12b).

(d) Surface modification of particles through partial contact with reactive media

This last route consists of arranging precursor particles along the interface between two media. Reacting molecules or particles are dissolved in the first medium, whereas the second is inert. Using air/liquid and liquid/solid interfaces, polymer particles were converted into half raspberry-like particles.³⁶ Schematic illustrations of the different processes used are provided on Fig. 13a. Polymer particles of controlled negative surface charge with a diameter of 1.5 μm have been first synthesized. Then, these particles were spread at an air/water interface in order to form a monolayer. While adjusting the pH of the subphase, the authors were able (i) to specifically hydrolyze the surface region dipping in the water phase and

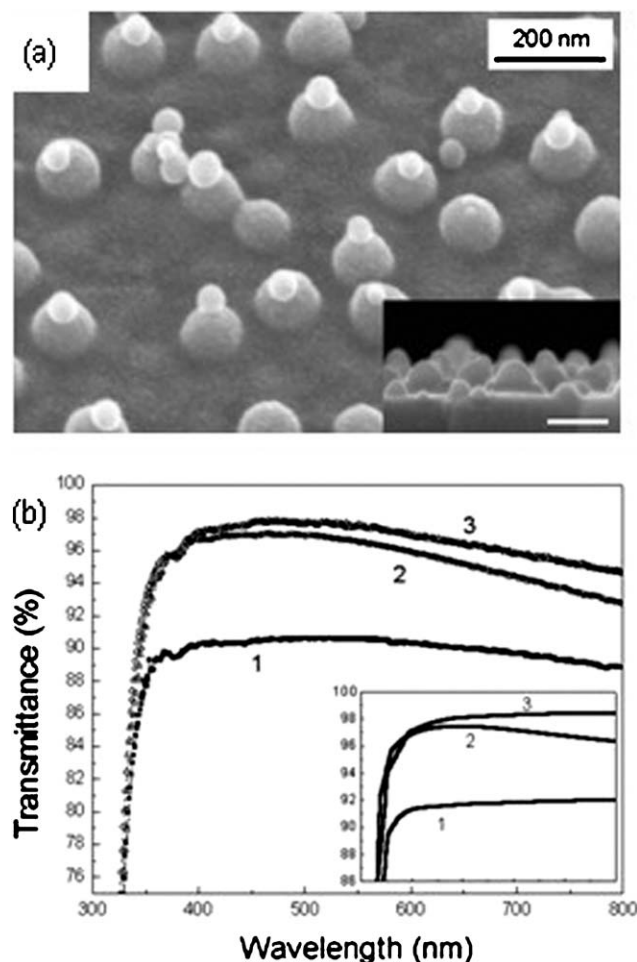


Fig. 12 (a) Field-emission scanning electron microscope images of a snowman-like particle array (inset: cross-sectional view; scale bar 100 nm). (b) Transmission spectra at normal incidence of uncoated glass (1), 100-nm particle monolayer (2) and snowman-like particle monolayer (3) (inset: simulated results; x-axis covers same wavelength range as main figure). Reprinted with permission from ref. 34.

subsequently immobilize human immunoglobulin G onto this hemisphere or (ii) to adsorb smaller latex particles (200 nm) of opposite charge initially dispersed in the water leading to dipolar particles. For the same last purpose, they also used a glass substrate as liquid/solid interface, onto which they transferred the previous monolayer of pristine particles prior to immersion in the dispersion of positively-charged latex particles. Due to steric hindrance limitations, they more successfully obtained half raspberry-like morphologies (Fig. 13b). Further experiments with similar goals were carried out by the same team using the Langmuir–Blodgett technique.³⁷ After spreading and compression at the air/water interface, a fluorine-containing (and consequently hydrophobic) terpolymer monolayer was transferred onto polymer particles (around 200 nm in diameter) previously deposited onto a glass substrate. Initially, the particles were hydrophilic due to the presence of amine groups at their surface and became amphiphilic after the transfer. To give evidence of the fact, contact angle measurement were carried out as well as X-ray photoelectron spectroscopy (XPS) analyses showing

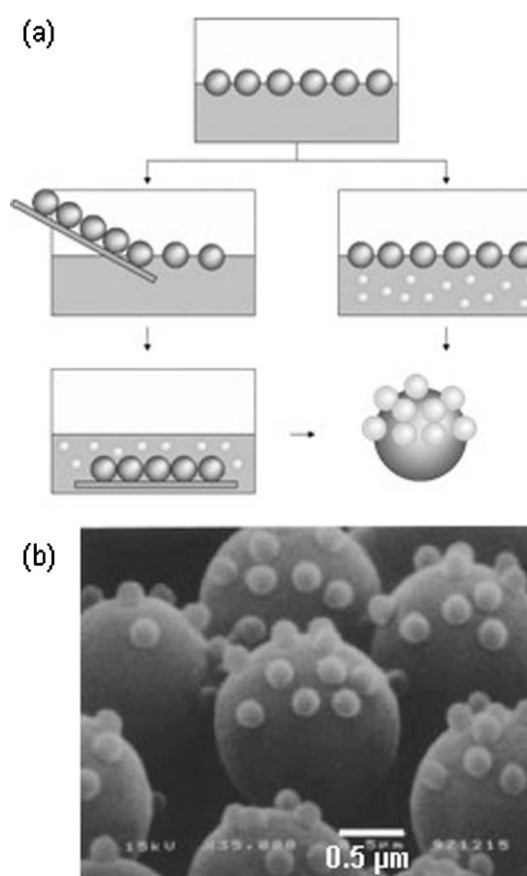


Fig. 13 (a) Schematic procedure of Janus particles preparation from precursor particles arranged along a liquid/solid interface (left route) or an air-liquid interface (right route). (b) Scanning electron microscopy image of half raspberry-like particles made of 2-μm reactive acrylic beads and 200-nm latex particles. Reprinted in part with permission from ref. 36. Copyright 1999 American Chemical Society.

that fluorine atoms were only present onto one hemisphere, the one being covered with the terpolymer.

A quite similar route was investigated for silica particles whose diameter was less than 100 nm.^{26,38} Taking advantage of both Langmuir techniques and chemical affinity between gold colloids and amine functions, silica nanoparticles were dis-symmetrically decorated by gold clusters (diameter close to 8–10 nm). Bare silica particles were surface-modified with amine functions through the grafting of aminopropyl-trimethoxysilane. These functionalized particles were then spread and packed tightly together at the surface of a Langmuir trough filled with a dilute solution of gold clusters. Transmission electron microscopy (TEM) observations clearly show that adsorption of metallic colloids only occurred onto the immersed surface of the precursor silica particle. Another route was investigated by transferring the monolayer of amino-functionalized silica nanoparticles onto solid substrates by the Langmuir–Blodgett technique and then immersing them in a solution of gold clusters. Attempts of statistical calculations from TEM micrographs, similar to those illustrated in Fig. 14, showed that whatever the technique employed, about 40% of the final silica particles were obviously dis-symmetrical, *i.e.*, with a gold coverage onto one single hemisphere.

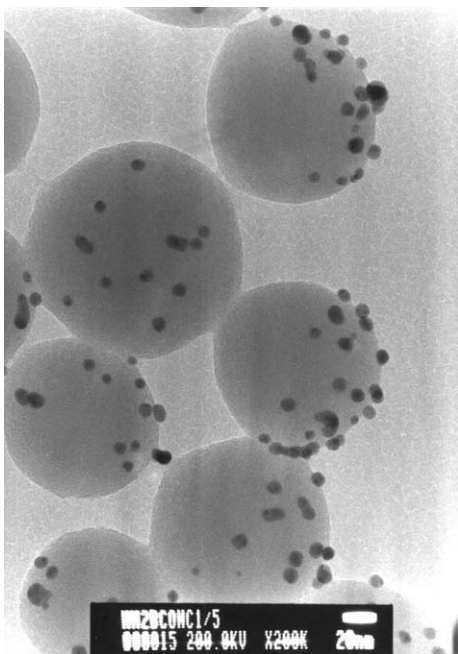


Fig. 14 TEM image showing 80-nm silica particles dis-symmetrically decorated by gold colloids. Such half raspberry-like morphologies were obtained by arranging a monolayer of aminated silica precursor particles at the surface of an aqueous colloidal dispersion of gold (scale bar: 20 nm). Reprinted with permission from ref. 38.

Nevertheless, about 30% extra appeared to be homogeneously covered and were in fact probably badly positioned onto the TEM grid. Lastly, 30% extra were too poorly covered (less than 5 gold colloids) to draw any conclusion.

(e) From plane to curved surfaces and interfaces

Every synthetic route previously described allowed the preparation of well-defined Janus particles with respect to their morphology and/or their surface functionalities. Nevertheless, one of the main drawbacks of such strategies is the low amount of produced particles by batch, which is probably the main limitation for further applications. In the current state of the art, a rough calculation allows us to evaluate the maximum number of Janus particles which can be prepared, either in a reasonable duration for the laser-induced technique, or assuming a reacting surface of 1 m² in all the other reported techniques. These values depend also on the size of the precursor particles as already discussed (Fig. 15). In the case of the laser technique, which operates particle by particle, only few tens of particles may be fabricated. In the other cases, the values are inversely proportional to the particle size, because all these techniques use one monolayer of particles. Nevertheless, it is important to point out that, assuming a medium density of 2, 10⁹ particles with a diameter of 100 μm weight around 1 kg, but 10¹⁸ particles with a diameter of 1 nm weight only about 1 mg. So, the industrial future of these routes will mainly depend on the development of processes involving surfaces or interfaces of very large area. One of the most promising outcomes will mainly be the use of emulsions or microparticulate solid substrates. Indeed, for a perfect

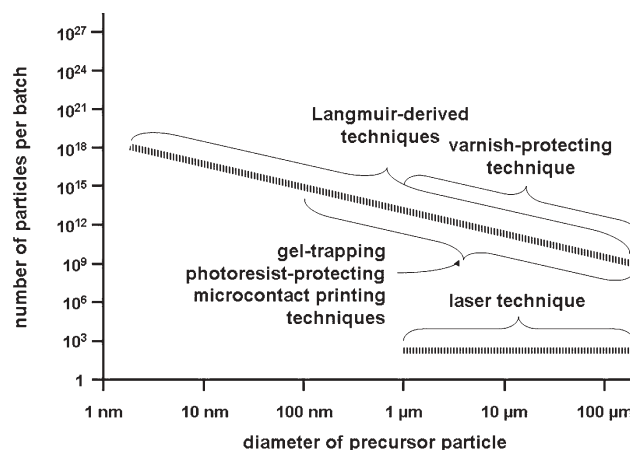


Fig. 15 Rough calculations of the maximum number of particles able to be dis-symmetrised according to the used techniques and the size of the precursor particles, assuming a reactor surface of 1 m².

dis-symmetry, the interface has to be theoretically infinitely flat. But, for the dis-symmetrisation of nanoparticles, it is reasonable to anticipate that closed interfaces or surfaces, such as those of droplets or particles of few tens of micrometers in diameter, would be promising tools, because the working area for dis-symmetrisation would be far higher.

First experiments were performed with 12-nm particles of a commercial grade of fumed silica previously made hydrophobic by surface treatment with trimethylalkoxysilane.³⁹ They were used to stabilise water-in-oil emulsion based on 50/50 toluene and alkaline water. The author assumed that the alkaline hydrolysis of Si–C bonds occurred essentially onto the surface of the particle hemisphere which was in contact with the aqueous phase, leading to the local regeneration of hydrophilic Si–OH or Si–O[−] groups. Thanks to sedimentation tests, it was observed that the higher the pH, the longer the emulsion stability. A Janus morphology was put forward to explain the stabilising effect of the particles. A similar strategy was recently patented.⁴⁰ However, the success of the dis-symmetrisation was also difficult to check and was only inferred from macroscopic properties such as the ability of these Janus nanoparticles to stabilize further emulsion with an improved efficiency.

Following a similar emulsion-based route, the synthesis of snowman-like particles made of two different materials was recently reported.⁴¹ The precursor nanoparticles, *e.g.*, Fe₃O₄, FePt or Au, were dispersed in a proper organic solvent, prior to their addition into an aqueous solution of silver nitrate. Ultrasonic emulsification afforded a stable oil-in-water emulsion. The reduction of silver cations occurred rapidly and essentially onto the particle surface leading to the nucleation and growth of one silver particle per precursor particle (Fig. 16). The reaction kinetics appeared to be easy to control, allowing generating snowman-like morphologies with different size ratios. The authors also checked that a discriminatory chemistry is also possible on each component of the resulting Janus particles.

Another example concerns the use of solidified droplets of paraffin as dis-symmetrisation surface.⁴² The primary

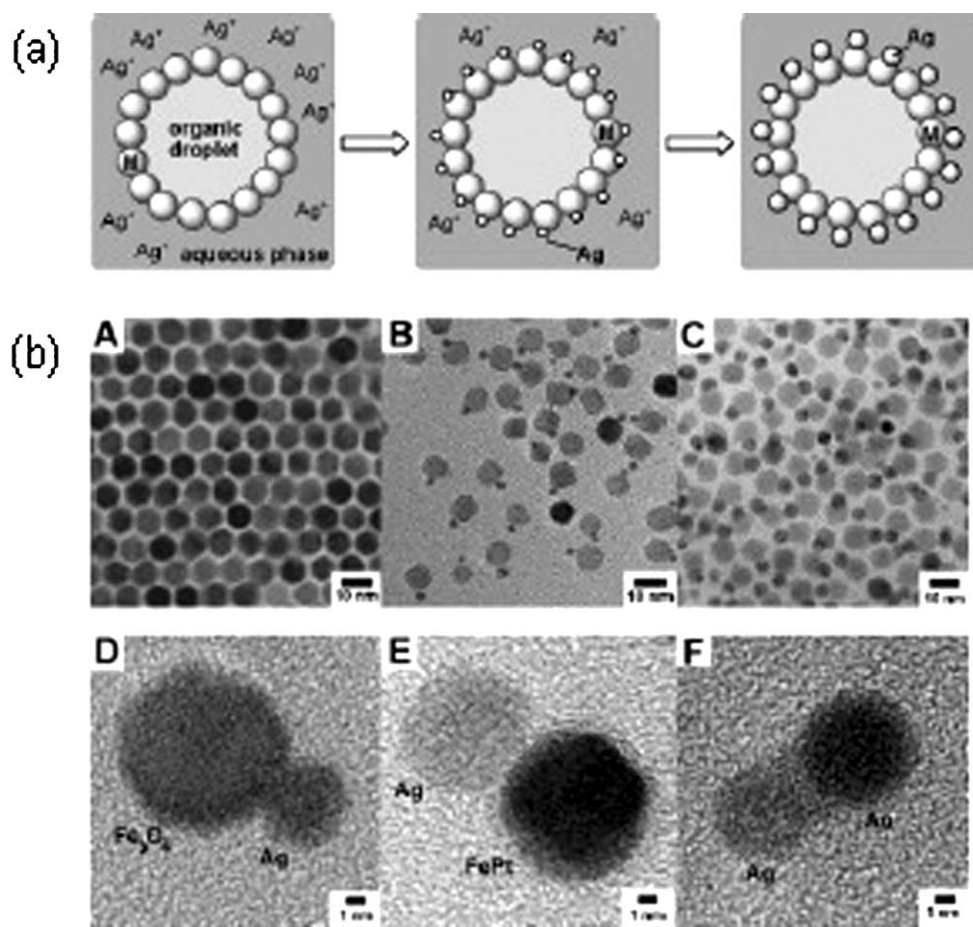


Fig. 16 (a) Schematic representation of the nucleation and growth of silver colloids onto particle at the surface of oil droplets. (b) TEM images of the precursor Fe_3O_4 particles (A), snowman-like Fe_3O_4 -Ag particles after 10 min reaction (B) and 30 min reaction (C) and high resolution TEM images of snowman-like particles based on Fe_3O_4 -Ag (D), FePt -Ag (E) and Au -Pt (F). Reprinted with permission from ref. 41. Copyright 2005 American Chemical Society.

emulsion was prepared at 60 °C from paraffin wax (melting point: 42–44 °C), water and 2- μm aminated silica particles under vigorous stirring at 9000 rpm for 1 min leading to average droplet size of about 100 μm . At room temperature, paraffin droplets solidified leading to the partial embedding of silica particles (Fig. 17a). The toposselective surface modification of the aminated silica particles was performed with the isothiocyanate derivative of fluorescein (FITC). The labelling of the free hemisphere of the particles was checked by confocal fluorescence microscopy (Fig. 17b) and flux cytometry. Indeed, the intensity of the fluorescence signal of supposed Janus particles was found just half that of isotropic silica particles of same size exposed to the fluorophore for the same duration.

Also concerning the use of microparticles as solid substrates for making dis-symmetrical nanoparticles, recent results showed that this route is conceivable at the expense of a great number of chemical steps and washing steps.⁴³ Preliminary experiments concerned the use of commercial trityl resins, formyl PS and poly(methyl methacrylate) (PMMA) beads. The first step consisted in the covalent grafting of amino-functionalized silica nanoparticles (100–200 nm in diameter) at their surface. After a thorough washing, these raspberry-like

particles were stirred in a gold colloidal solution and washed again. The more delicate step concerned the cleavage reactions for removing the gold-decorated silica particles. The best

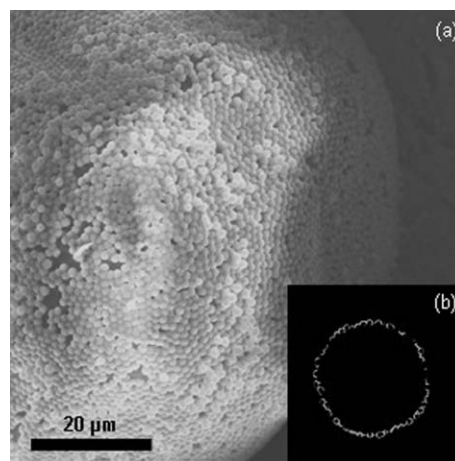


Fig. 17 (a) SEM image of a solidified paraffin droplet stabilized by 2- μm aminated silica particles. (b) Confocal fluorescence microscopy image of a solidified paraffin droplet stabilized by 2- μm aminated silica particles after FITC labelling.

results were obtained with the PMMA beads, which were destroyed through a heat treatment at 300 °C overnight, during which they slowly depolymerised leading to gaseous monomers.

4 Processes based on template-directed self-assembly of particles

Snowman-like, dumbbell-like or half raspberry-like particles could also be obtained by assembling preformed precursor particles. In the self-assembling approach, the precursor particles assemble following their favoured ways of either minimum local or global energy or favoured kinetics achieving supraparticles of robust mechanical stability.⁴⁴ The use of templates with defined dimensions and complexities provide the opportunities to program self-assembly of the components. Using lithographic techniques, 1-D or 2-D templates may be generated and the achievement of minimum feature sizes of around 10 nm is anticipated in the next decade. In this section, only the template-directed colloidal self-assembly techniques allowing the association of particles of different bulk and/or surface natures, comparable to Janus particles, will be mentioned.

A first method used simultaneously geometrical confinement and attractive capillary forces through the dewetting of an aqueous dispersion of spherical particles previously confined within a parallel cell composed of two glass substrates (Fig. 18a).⁴⁵ The surface of the bottom substrate has been patterned with a 2-D array of cylindrical holes. When this dispersion was allowed to dewet slowly across the cell, the capillary force exerted on the rear edge of this liquid 'slug' would drag the spherical particles across the surface of the bottom substrate until they were physically trapped in the hole arrays. The maximum number of particles that could be retained in each hole was determined by the ratio between the dimensions of the holes and the diameter of the particles. In order to create snowman-like assemblies, the first precursor particles are fixed in the holes by heating at a temperature slightly higher than the glass transition temperature of the particles and then a dispersion of the smaller precursor particles is introduced in the same cell. When assembled in each hole, both particles may be welded into a single piece by heating (Figs. 18b–c) and then released by dissolving the photoresist pattern in ethanol under sonication.

A second method concerns the deposition of a single gold nanoparticle or nanowire on aminated silica particle using a microporous membrane as template.⁴⁶ The diameter of the silica precursor particles exceeded that of the membrane pores by one order of magnitude and allowed to seal one pore. When a dispersion of gold colloids is filtered through the membrane, one or several gold nanoparticles are trapped in this pore and adsorbed onto the silica particle, leading to snowman-like and comparable assemblies which were released by sonicating the membrane filter.

If these template-directed colloidal self-assembly strategies lead to well-defined supraparticles and open avenues to imaginative scientists, their current low yield and high cost due to the template fabrication shall be also mentioned.

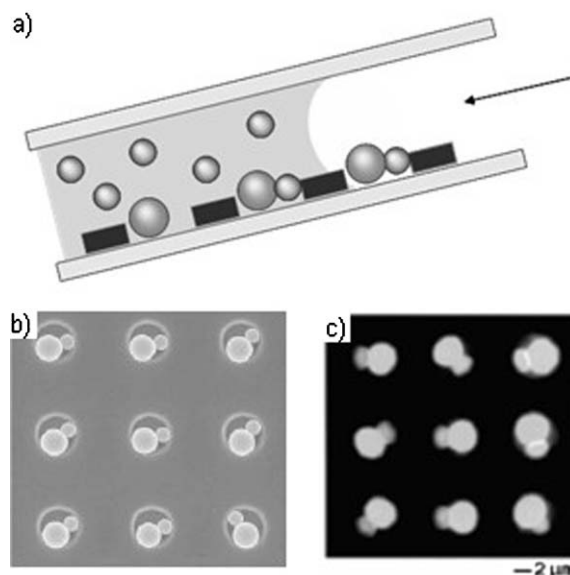


Fig. 18 (a) Schematic representation of the experimental cell and procedure for the dewetting on the second particle dispersion. (b) SEM images of a 2-D array of hybrid snowman-like particles made of 2.8-μm PS beads and 1.6-μm silica particles. (c) Fluorescence microscopy image of a 2-D array of snowman-like particles self-assembled from 3.0-μm and 1.7-μm PS beads doped with fluorescein and rhodamine, respectively. The green and red dyes were selectively excited and recombined into an overlapped image. Reprinted with permission from ref. 45. Copyright 2001 American Chemical Society.

5 Processes based on controlled phase separation phenomena

(a) Chemical reactions or crystallisation within core-shell inorganic particles

In this section, Janus nanoparticles are obtained when pre-formed core-shell nanoparticles are forced into phase separation simultaneously or subsequently to a chemical reaction with one component.

A first example concerned the reaction of Ag-silica nanoparticles with molecular iodine I₂, which is a strong oxidant in particular towards metallic silver.⁴⁷ The precursor core-shell particles were prepared from Ag nanoparticle dispersions and tetraethylorthosilicate.⁴⁸ In such conditions, the silica shell is known to be microporous. Therefore, chemical exchanges between Ag cores and iodine were possible. Indeed, the evolution of the absorbance spectrum of the dispersion showed the disappearance of the Ag surface plasmon absorption band at 390 nm and the appearance of the typical 420 nm excitation peak of colloidal β-AgI. Because of the presence of the silica shell, the reaction rate was slow enough to monitor by TEM the evolution of the particle morphology (Fig. 19). It was observed a rapid evolution from the Ag-silica core-shell morphology to AgI-silica snowman-like morphology. A mechanism was proposed involving the temporary existence of a single AgI filament between the Ag core and the AgI growing particle onto the silica surface.

By taking advantage of lattice mismatching and selective annealing, the synthesis of FePt–CdS snowman-like particles was reported.⁴⁹ Amorphous CdS was deposited in two steps on

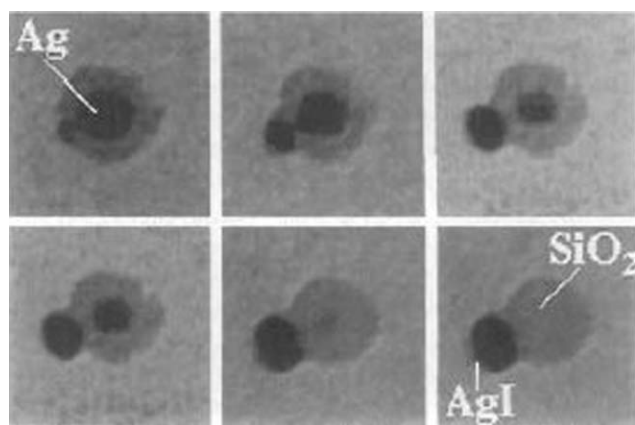


Fig. 19 TEM images of a single 30-nm Ag-silica particle as a function of the time after exposure to 2 mM I_2 . The final image was taken about 20 min after the first one. Reprinted with permission from ref. 47.

the surface of FePt nanoparticles to form metastable core-shell structures, in which CdS crystallised upon heating on the occasion of a third step (Fig. 20a). The spontaneous core-shell-to-snowman evolution was explained as the result of (i) the incompatibility of the FePt and CdS lattices and (ii) the surface tension when they are dispersed in a liquid, *i.e.*, dioctyl ether (dewetting phenomenon). The final Janus particles had sizes less than 10 nm (Fig. 20b) and exhibited both superparamagnetism and fluorescence.

(b) Phase separation phenomena in seeded emulsion polymerisation

Emulsion polymerization is an heterophase polymerization process of great industrial importance allowing the elaboration

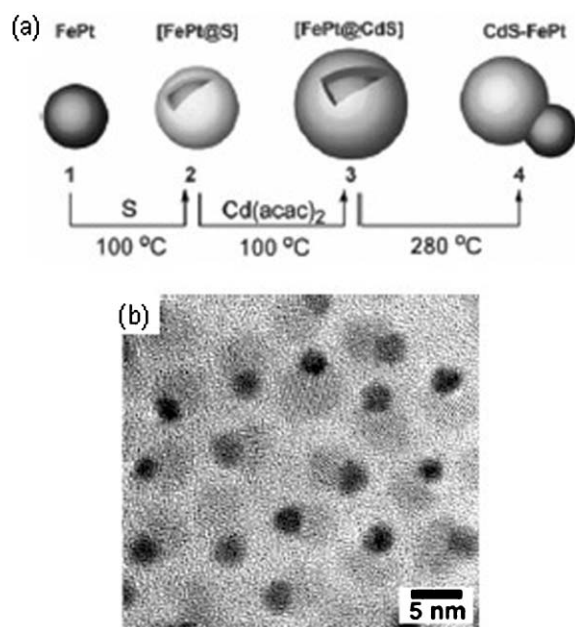


Fig. 20 (a) Schematic representation of the synthesis of CdS-FePt snowman-like particles. (b) High-resolution TEM image of CdS-FePt snowman-like particles. Reprinted in part with permission from ref. 49. Copyright 2004 American Chemical Society.

of stable colloidal dispersions of latex polymer particles in water. In “conventional” emulsion polymerization, the polymer particles are formed by starting from an insoluble (or scarcely soluble) monomer emulsified by the aid of a surfactant above its critical micelle concentration (CMC). The monomer is originally distributed between coarse emulsion droplets, surfactant micelles and the water phase where a small proportion of monomer (depending on its solubility) is molecularly dissolved. Polymerization starts in the aqueous phase by the formation of free radicals through the initiator thermolysis and the addition of the first monomer units. These oligomeric radical species are rapidly captured by the monomer-swollen micelles, where propagation is supported by absorption of monomer diffusing from the monomer droplets through the aqueous phase to maintain equilibrium. Therefore, stabilized nuclei are produced leading to primary particles, growing gradually until the monomer is completely consumed. The size of these particles is determined by the number of primary latex particles formed and the time during which they grow. The polymer particles generally have final diameters in the range 0.05–1 μm . One of the important features of emulsion polymerization is also the ability to control particle morphology, *e.g.*, formation of core-shell particles and other equilibrium morphologies by successive additions of different monomers.

In particular several authors have studied the formation of dis-symmetrical morphologies as the consequence of phase separation phenomena during some growth-seeded polymerization processes.^{50,51,52} Theoretical explanations taking into account geometrical as well as thermodynamical considerations were proposed to predict the final particle morphology.⁵¹ In general, the dumbbell-like, snowman-like or acorn-like observed morphologies were in agreement with a thermodynamic model giving the chemical potential of the monomers in the swollen particle as the sum of three components. First, the monomer-polymer mixing force, promoting particle expansion and depending on the volume fraction of polymer in the swollen particle and the monomer-polymer interaction parameter. Second, the polymer network elastic-retractile force (influenced by temperature and degree of cross-linking in the seeds) and third, the water-particle interfacial tension (related to the seed size) that restrict particle expansion. On the whole, the phase separation process was favoured by increasing either the monomer/polymer swelling ratio or the seed cross-link density or the seed size or the temperature or the cross-linker rate in the mixture of swelling monomers, *etc.* In many cases, the chemical natures of the two components were quite similar and that is why they cannot really be considered as Janus particles.

Nevertheless, 130-nm acorn-like nanoparticles with a soft poly(*n*-butyl acrylate) core partially capped with hard PMMA through successive MMA emulsion polymerization reactions were reported.⁵² Atomic force microscopy experiments in tapping mode were carried out and gave evidence for a preferential oriented adsorption of the particles when deposited from a dilute dispersion onto flat substrates. On hydrophilic surfaces, *e.g.*, muscovite mica, the hard phase is preferentially oriented toward the substrate, whereas on hydrophobic substrates, *e.g.*, *n*-octadecyltrichlorosilane-treated

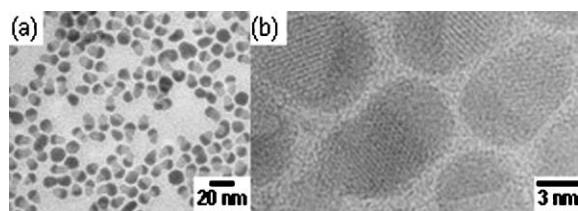


Fig. 21 (a) TEM image and (b) high-resolution TEM image of acorn-shaped $\text{PdS}_x/\text{Co}_9\text{S}_8$ particles. Reprinted in part with permission from ref. 53. Copyright 2004 American Chemical Society.

silica, the soft phase is preferentially oriented toward the surface.

6 Processes based on controlled surface nucleation

The last known strategy to fabricate Janus nanoparticles in the shape of dumbbells, snowmen or acorns is based on the controlled nucleation and growth of a single particle onto the surface of a precursor. These routes are not assisted by reactive interfaces or directional fluxes and, in general, the 1 : 1 particle ratio is statistically controlled.

Bicompartamental acorn-shaped $\text{PdS}_x\text{-Co}_9\text{S}_8$ particles were obtained by reduction of $\text{Co}(\text{acac})_2 \cdot 2\text{H}_2\text{O}$ and $\text{Pd}(\text{acac})_2$ with 1,2-hexadecanediol in di-*n*-ocyl ether in the presence of 1-octadecanethiol.⁵³ As shown by TEM on Fig. 21, acorn-like particles were predominantly observed together with a minor fragment of spherical Pd sulfide particles. The presence of a thiol derivative is mandatory, leading to the formation of metal sulfides by the spontaneous cleavage of the C–S bonds. Thanks to spectroscopic analyses and TEM observations, mechanism was speculated and could be summarised by the following main stages: (i) the reduction of Pd(II) ions by 1-octadecanethiol to yield $\text{Pd}_n(\text{SC}_{18}\text{H}_{37})_m$ clusters, (ii) their conversion into PdS_x nanoparticles still stabilised by chemisorbed 1-octadecanethiol and (iii) nucleation and growth of the Co_9S_8 phase along the [001] direction. The acorn formation would be the consequence of the Pd surfaces requirement for producing the free sulfur atoms and supplying them to the cobalt phases.

Dumbbell-like $\text{Au-Fe}_3\text{O}_4$ nanoparticles were synthesized using decomposition of $\text{Fe}(\text{CO})_5$ on the surface of gold precursor nanoparticles followed by oxidation in 1-octadecene solvent.⁵⁴ The dumbbells were formed through epitaxial growth of iron oxide on the gold seeds (Fig. 22) and it was

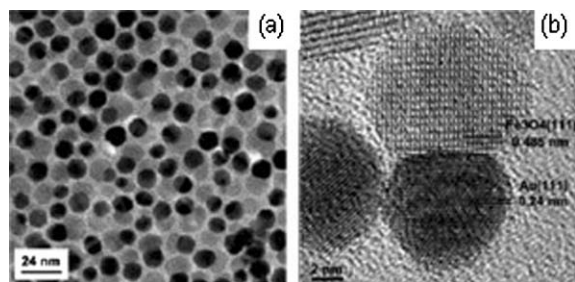


Fig. 22 (a) TEM image and (b) high-resolution TEM image of dumbbell-like $\text{Au-Fe}_3\text{O}_4$ nanoparticles. Reprinted in part with permission from ref. 54. Copyright 2005 American Chemical Society.

shown that the growth can be affected by the solvent polarity (for instance the use of diphenyl ether resulted in flower-like morphologies). The particles simultaneously displayed the characteristic surface plasmon absorption of gold and the magnetic properties of Fe_3O_4 . Those properties are altered by the interactions between the two components. Quite similar morphologies were observed on the occasion of the sequential reduction of AgNO_3 and Na_2SeO_3 in ascorbic acid aqueous solutions.⁵⁵ By adjusting the concentration of selenium ions, the ratio of Ag nanoparticles to Se nanoparticles was controlled from 1 : 1 to 1 : 3 leading in particular to snowman-like Ag–Se nanoparticles.

A last series of examples deals with the synthesis of hybrid Janus nanoparticles through controlled surface-nucleation of latex particles onto inorganic nanoparticles. This route is also derived from the growth-seeded emulsion polymerisation technique, but differs from the strategy described in the previous section by the fact that the seeds are inorganic particles. Indeed, they are neither able to be swelled by monomers nor deformable. Therefore, only surface interactions can be provided towards organic monomers and/or oligomeric radical species leading to latex surface nucleation. Nevertheless, the surface of inorganic particles is generally too hydrophilic for generating spontaneous interactions. It is well-known that the encapsulation of inorganic particles by polymer coating (core-shell morphology) through emulsion polymerisation-derived techniques necessitates the preliminary seed surface modification by molecular agents able to promote favourable interactions.⁵⁶ Nevertheless, when the surface is only moderately modified, the capture of the oligomeric radical species by the inorganic surface is possible but the latex particles grow independently, since the wetting is not efficient enough. Such a behavior was observed when silica seeds were previously let to react with a monomethylether mono methylmethacrylate poly(ethylene oxide) macro-monomer ($1.5 \mu\text{mole.m}^{-2}$) prior to styrene emulsion polymerization.⁵⁷ Because of the large size of silica seeds (500 nm), raspberry-like silica-PS particles were obtained. But the average number of polystyrene nodules per silica particle can be tuned by varying the diameter and the concentration of the silica seeds, which is to say, by adjusting the particle number ratio $N_{\text{latex}} : N_{\text{silica}}$.⁵⁸ When this ratio is equal to 1 : 1, original dumbbell-like or snowman-like morphologies were obtained in yields higher than 70% with respect to silica seeds. This strategy was successfully applied to silica seeds with diameter from 50 to 150 nm (Fig. 23). Similar results were obtained when silica seeds were previously treated with small amounts

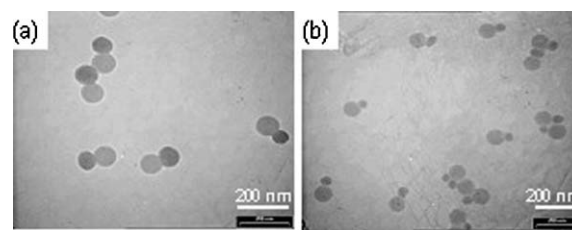


Fig. 23 TEM image of dumbbell-like silica-PS particles obtained by latex surface nucleation on silica particles with an initial diameter of (a) 80 nm and (b) 50 nm.

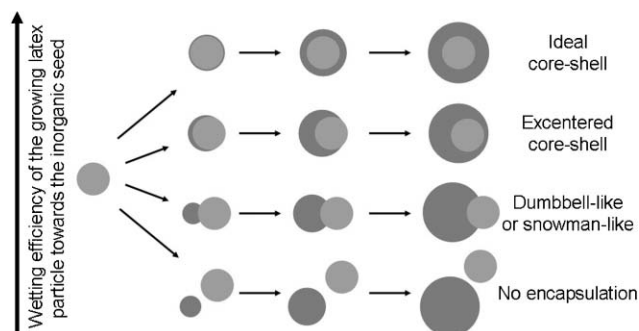


Fig. 24 Schematic morphology evolution of inorganic cores by latex particles as a function of their respective affinities (cross sections).

of methacryloxymethyltriethoxysilane (in the range 0.1–1 molecules per nm^2).⁵⁹ In this case, it was shown that the higher the silane surface density, the more encapsulating the PS latex particle. So, by controlling experimental parameters such as the nature and surface density of promoting agents, the nature of surfactants, the particle number ratio, *etc.*, it would be conceivable to design a large panel of hybrid Janus particles (Fig. 24). Nevertheless, no theoretical aspect on these morphology developments has been reported so far. It seems that they would be governed by the balance between the interfacial energies and the driving force of the latex particles' growth. Such a theoretical study could be inspired by the recent and original numerical study of a hard sphere wetted by a spherical viscoelastic particle, according to a Monte Carlo approach.⁶⁰

Lastly, the same authors demonstrated that these silica–PS particles obtained in the shape of hybrid dumbbells or snowmen may be powerful intermediate structures for designing Janus particles according to an original latex protection/deprotection strategy (Fig. 25).⁶¹ Indeed, it was observed that the interactions between silica particles and PS nodules may be disrupted under mild ultrasonication conditions or by ultracentrifugation in an aqueous solution of sodium dodecyl sulfate. This multi-step route is similar to the previously reported varnish-protecting, gel-trapping or photoresist-protecting techniques, but differs by the fact that here each particle carries its own mask. Therefore, no infinitely plane surface is necessary and all the chemical reactions can be performed in conventional reactors. According to this route,

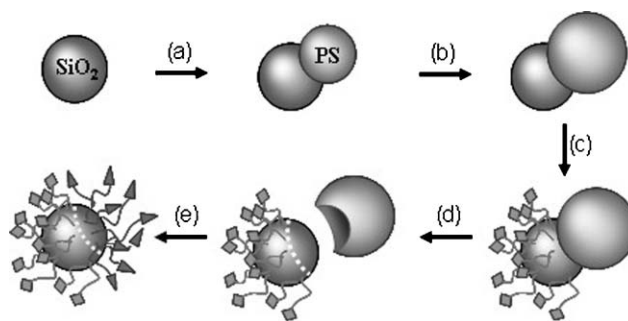


Fig. 25 Schematic representation of the consecutive stages for the fabrication of the Janus particles through the latex protection/deprotection strategy: (a) nucleation of a single PS nodule, (b) growth of this PS nodule until the desired silica surface is masked, (c) chemical modification of the free silica surface by a first reagent, (d) latex removing by ultrasonication or ultracentrifugation and (e) chemical modification of the released silica surface by a second reagent.

Janus silica nanoparticles with a methylated hemisphere and an aminated hemisphere were successfully fabricated.

7 Conclusion

Since the pioneering work of De Gennes and his colleagues, numerous original routes have been developed for the synthesis of Janus particles (Fig. 26). They are one of the fruits of the remarkable progress which has been achieved in both polymer and inorganic chemistry yielding well-defined particles from the viewpoint of their size, their shape and their surface chemistry. In particular, Janus particles are now available in the size range of a few nanometers, *i.e.*, five thousand times smaller than the pioneering Janus glass beads. Anyway, the dis-symmetry checking of these nanoparticles is not a simple task and, even if TEM and high-resolution TEM are now common imaging techniques, they are not usable for evidencing Janus particles whose difference between both hemispheres is at the molecular level. In those last cases, an interesting but largely unanswered problem concerns the surface mobility of ligands, which could lead to ligand exchanges and tend to their isotropic arrangements. If the reported works did not mention the instability of the Janus-like character, no systematic study was focused on such aspects.

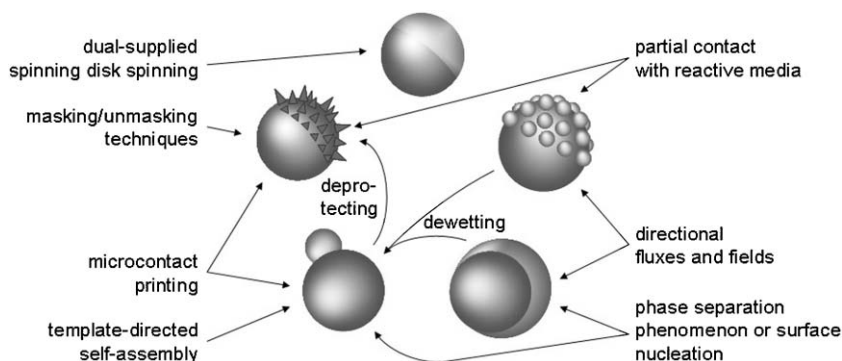


Fig. 26 Schematic representation of the synthetic routes yielding Janus particles.

Some of the suspected properties of Janus nanoparticles have now been checked: their ability to stabilise oil-in-water or water-in-oil emulsions, to orient themselves in electric fields, to be toposelectively surface modified for dual-functionalised devices, to be used as building blocks for supraparticular assemblies, etc.

Their potential application fields are numerous, but further efforts shall be done to develop robust and reliable strategies that can be extrapolated to large scale productions. Current or future routes based on controlled phase separation and nucleation phenomena will very probably be more appropriate from the viewpoint of their yield and cost.

Lastly, a special emphasis shall be done to hybrid organic–inorganic Janus particles, because (i) the chemistries of both counterparts are very different and complementary, (ii) they will allow to combine properties of polymeric and mineral materials and (iii) the interactions between both components may be easily tuned and in particular made reversible.

Acknowledgements

The authors are very grateful to Christophe Mingotaud, Laetitia Petit, Céline Poncet-Legrand, Pascale Hazot, Franck Pereira, Marie-Hélène Delville, Anne-Françoise Mingotaud, Vincent Léon, Elisabeth Sellier, Corinne Coudun, Alexandra Cruaux, Jean-Pierre Manaud, Fabrice Meunier, Pierre Dubergé, Béatrice Agricole and Michel Martineau for valuable collaboration and helpful discussions. Their own work was supported in part by the French Ministry of Education, Research and Technology (Action Concertée Incitative «Jeunes Chercheurs» – Appel d'offre 1999) and the Conseil Régional d'Aquitaine.

References

- 1 C. N. R. Rao and K. A. Cheetham, *J. Mater. Chem.*, 2001, **11**, 2887–2894; S. Mornet, S. Vasseur, F. Grasset and E. Duguet, *J. Mater. Chem.*, 2004, **14**, 2161–2175; Y. Xia and N. J. Halas, *MRS Bull.*, 2005, **30**, 338–343.
- 2 R. A. Vaia and H. D. Wagner, *Mater. Today*, 2004, **7**, 32–37.
- 3 C. J. Murphy, *Science*, 2002, **298**, 2139–2141; N. R. Jana, L. Gearheart and C. J. Murphy, *J. Phys. Chem. B*, 2001, **105**, 4065–4067; R. Jin, Y. W. Cao, C. A. Mirkin, K. L. Kelly, G. C. Schatz and J. G. Zheng, *Science*, 2001, **294**, 1901–1903.
- 4 P. G. De Gennes, *Croat. Chim. Acta*, 1998, **71**, 833–836.
- 5 P. G. De Gennes, *Rev. Mod. Phys.*, 1992, **64**, 645–648.
- 6 C. Casagrande, P. Fabre, E. Raphaël and M. Veyssié, *Phys. Lett.*, 1989, **9**, 251–255.
- 7 T. Ondarçuhu, P. Fabre, E. Raphaël and M. Veyssié, *J. Phys. France*, 1990, **51**, 1527–1536.
- 8 K. L. Wooley, C. J. Hawker and J. M. J. Fréchet, *J. Am. Chem. Soc.*, 1993, **115**, 11496–11505; V. Heroguez, Y. Gnanou and M. Fontanille, *Macromolecules*, 1997, **30**, 4791–4798; N. Hadjichristidis, M. Pitsikalis, S. Pispas and H. Latrou, *Chem. Rev.*, 2001, **101**, 3747–3792.
- 9 R. Saito, A. Fujita, A. Ichimura and K. Ishizu, *J. Polym. Sci., Part A: Polym. Chem.*, 2000, **38**, 2091–2097; H. Xu, R. Erhardt, V. Abetz, A. H. E. Müller and W. A. Goedel, *Langmuir*, 2001, **17**, 6787–6793; R. Erhardt, A. Böker, H. Zettl, H. Kaya, W. Pyckhout-Hintzen, G. Krausch, V. Abetz and A. H. E. Müller, *Macromolecules*, 2001, **34**, 1069–1075; H. Kaya, *Appl. Phys. A*, 2002, **74**, S507–S509; R. Erhardt, M. Zhang, A. Böker, H. Zettl, C. Abetz, P. Frederik, G. Krausch, V. Abetz and A. H. E. Müller, *J. Am. Chem. Soc.*, 2003, **125**, 3260–3267; Y. Liu, V. Abetz and A. H. E. Müller, *Macromolecules*, 2003, **36**, 7894–7898; T. Fütterer, G. A. Vliegthart and P. R. Lang, *Macromolecules*, 2004, **37**, 8407–8413; C. A. Fustin, V. Abetz and J. F. Gohy, *Eur. Phys. J. E*, 2005, **6**, 291–302.
- 10 S. Reculosa, C. Mingotaud, E. Duguet and S. Ravaine, *Dekker Encyclopedia of Nanoscience and Nanotechnology*, edited by J.A. Schwarz, C.I. Contescu and K. Putyera, (Marcel Dekker Inc), 2004, pp. 943–953.
- 11 B. P. Binks, *Curr. Opin. Colloid Interf. Sci.*, 2002, **7**, 21–41.
- 12 S. U. Pickering, *J. Chem. Soc.*, 1907, **91**, 2001.
- 13 B. P. Binks and S. O. Lumdson, *Langmuir*, 2000, **16**, 2539–2547; B. P. Binks and S. O. Lumdson, *Langmuir*, 2000, **16**, 8622–8631.
- 14 B. P. Binks and P. D. I. Fletcher, *Langmuir*, 2001, **17**, 4708–4710.
- 15 H. Takei and N. Shimizu, *Langmuir*, 1997, **13**, 1865–1868.
- 16 N. K. Sheridan, E. A. Richley, J. C. Mikkelsen, D. Tsuda, J. M. Crowley, K. A. Oraba, M. E. Howard, M. A. Rodkin, R. Swidler and R. Sprague, *Proceeding of the IDRC, SID/IEEE*, September 1997, Toronto, Canada.
- 17 For more details, see <http://www.gyriconmedia.com/> (accessed June 2005).
- 18 C. Casagrande and M. Veyssié, *C.R. Acad. Sci. Paris*, 1988, **306**, 1423–1425.
- 19 E. Raphaël, *C.R. Acad. Sci. Paris*, 1988, **307**, 9–12.
- 20 Y. Nonomura, S. Komura and K. Tsujii, *Langmuir*, 2004, **20**, 11821–11823.
- 21 Z. Bao, L. Chen, M. Weldon, E. Chandross, O. Cherniavskaya, Y. Dai and J. B. H. Tok, *Chem. Mater.*, 2002, **14**, 24–26.
- 22 V. N. Paunov, *Langmuir*, 2003, **19**, 7970–7976.
- 23 V. N. Paunov and O. J. Cayre, *Adv. Mater.*, 2004, **16**, 788–791.
- 24 J. Choi, Y. Zhao, D. Zhang, S. Chien and Y.-H. Lo, *Nano Lett.*, 2003, **3**, 995–1000.
- 25 M. Himmelhaus and H. Takei, *Sens. Actuators B*, 2000, **63**, 24–30.
- 26 L. Petit, J.-P. Manaud, C. Mingotaud, S. Ravaine and E. Duguet, *Mater. Lett.*, 2001, **51**, 478–484.
- 27 Y. Lu, H. Xiong, X. Jiang and Y. Xia, *J. Am. Chem. Soc.*, 2003, **125**, 12724–12725.
- 28 J. C. Love, B. D. Gates, D. B. Wolfe, K. E. Paul and G. M. Whitesides, *Nano Lett.*, 2002, **2**, 891–894.
- 29 M. G. Bajaj and P. E. Laibinis, *Molecular Engineering of Biological and Chemical Systems*, Janv. 2004, accessible at <http://hdl.handle.net/1721.1/3947>; M. G. Bajaj and P. E. Laibinis, *Mater. Res. Soc. Symp. Proc.*, 2004, **EXS-1**, H1.2.1–H1.2.3.
- 30 J. C. Bradley and Z. Ma, *Angew. Chem. Int. Ed.*, 1999, **38**, 1663–1666.
- 31 E. Hugonnot, A. Carles, M.-H. Delville, P. Panizza and J.-P. Delville, *Langmuir*, 2003, **19**, 226–229.
- 32 O. Cayre, V. N. Paunov and O. D. Velev, *Chem. Commun.*, 2003, **18**, 2296–2297.
- 33 O. Cayre, V. N. Paunov and O. D. Velev, *J. Mater. Chem.*, 2003, **13**, 2445–2450.
- 34 H. Y. Koo, D. K. Yi, S. J. Yoo and D. Y. Kim, *Adv. Mater.*, 2004, **16**, 274–277.
- 35 A. Gombert, W. Glaubbitt, K. Rose, J. Dreiholz, B. Bläsi, A. Heinzl, D. Sporn, W. Döll and V. Wittwer, *Thin Solid Films*, 1999, **351**, 73–78; C. Aydin, A. Zaslavsky, G. J. Sonek and J. Goldstein, *Appl. Phys. Lett.*, 2002, **80**, 2242–2244.
- 36 K. Fujimoto, K. Nakahama, M. Shidara and H. Kawaguchi, *Langmuir*, 1999, **15**, 4630–4635.
- 37 K. Nakahama, H. Kawaguchi and K. Fujimoto, *Langmuir*, 2000, **16**, 7882–7886.
- 38 L. Petit, E. Sellier, E. Duguet, S. Ravaine and C. Mingotaud, *J. Mater. Chem.*, 2000, **10**, 253–254.
- 39 G. Rossmly, *Prog. Colloid Polym. Sci.*, 1998, **111**, 17–26.
- 40 J. Y. Chane Ching, *French Patent FR 2,808,704* (2001); J. Y. Chane Ching and D. Monin, *French Patent FR 2,832,076* (2004).
- 41 H. Gu, Z. Yang, J. Gao, C. K. Chang and B. Xu, *J. Am. Chem. Soc.*, 2005, **127**, 34–35.
- 42 S. Reculosa, *PhD Thesis, n°2807, Université Bordeaux-I, France*, 2003.
- 43 C. Poncet-Legrand, L. Petit, S. Reculosa, C. Mingotaud, E. Duguet and S. Ravaine, *Progr. Colloid Polym. Sci.*, 2004, **123**, 240–244.
- 44 D. Wang and H. Möhwald, *J. Mater. Chem.*, 2004, **14**, 459–468.
- 45 Y. Yin, Y. Lu and Y. Xia, *J. Am. Chem. Soc.*, 2001, **123**, 771–772; Y. Yin, Y. Lu, B. Gates and Y. Xia, *J. Am. Chem. Soc.*, 2001, **123**, 8718–8729; Y. Xia, Y. Yin, Y. Lu and J. McLellan, *Adv. Funct. Mater.*, 2003, **13**, 907–918.

- 46 L. Nagle and D. Fitzmaurice, *Adv. Mater.*, 2003, **15**, 933–935.
- 47 M. Giersig, T. Ung, L. M. Liz-Marzan and P. Mulvaney, *Adv. Mater.*, 1997, **9**, 570–575.
- 48 L. M. Liz-Marzan, M. Giersig and P. Mulvaney, *J. Chem. Soc., Chem. Commun.*, 1996, 731.
- 49 H. Gu, R. Zheng, X. Zhang and B. Xu, *J. Am. Chem. Soc.*, 2004, **126**, 5664–5665.
- 50 I. Cho and K. W. Lee, *J. Appl. Polym. Sci.*, 1985, **30**, 1903–1926; M. Okubo, T. Yamashita, H. Minami and Y. Konishi, *Colloid Polym. Sci.*, 1998, **276**, 887–892; H. R. Sheu, M. S. El-Aasser and J. W. Vanderhoff, *J. Polym. Sci., Part A: Polym. Chem.*, 1990, **28**, 653–667; H. Ni, G. Ma, M. Nagai and S. Omi, *J. Appl. Polym. Sci.*, 2000, **76**, 1731–1740.
- 51 Y. C. Chen, V. Dimonie and M. S. El-Aasser, *J. Appl. Polym. Sci.*, 1991, **42**, 1049–1063; Y. G. J. Durant and J. Guillot, *Colloid Polym. Sci.*, 1993, **271**, 607–615; Y. Duda and F. Vazquez, *Langmuir*, 2005, **21**, 1096–1102.
- 52 A. Pfau, R. Sander and S. Kirsch, *Langmuir*, 2002, **18**, 2880–2887.
- 53 T. Teranishi, Y. Inoue, M. Nakaya, Y. Oumi and T. Sano, *J. Am. Chem. Soc.*, 2004, **126**, 9914–9915.
- 54 H. Yu, M. Chen, P. M. Rice, S. X. Wang, R. L. White and S. Sun, *Nano. Lett.*, 2005, **5**, 379–382.
- 55 X. Gao, L. Yu, R. I. MacCuspie and H. Matsui, *Adv. Mater.*, 2005, **17**, 426–429.
- 56 E. Bourgeat-Lami and E. Duguet, in *Functional Organic Coating* edited by S.K. Ghosh (Wiley, 2005) in press.
- 57 S. Reculosa, C. Poncet-Legrand, S. Ravaine, C. Mingotaud, E. Duguet and E. Bourgeat-Lami, *Chem. Mater.*, 2002, **14**, 2354–2359.
- 58 S. Reculosa, C. Poncet-Legrand, S. Ravaine, E. Duguet, E. Bourgeat-Lami and C. Mingotaud, French Patent FR 2,846,572 WO 2004/044061 (2004); E. Duguet, S. Reculosa, A. Perro, C. Poncet-Legrand, S. Ravaine, E. Bourgeat-Lami and C. Mingotaud, *Mater. Res. Soc., Symp. Proc.*, 2005, **847**, EE1.1.1–10.
- 59 S. Reculosa, C. Poncet-Legrand, A. Perro, E. Duguet, E. Bourgeat-Lami, C. Mingotaud and S. Ravaine, *Chem. Mater.*, 2005, **17**, 3338–3344.
- 60 S. Bordère, *Composites: Part A*, 2002, **33**, 1355–1360.
- 61 E. Duguet, C. Poncet-Legrand, S. Ravaine, E. Bourgeat-Lami, S. Reculosa, C. Mingotaud, M.H. Delville and F. Pereira, French Patent FR 2,862,236 WO 2005/049195 (2005).